Materials Science-Poland, 39(3), 2021, pp. 331-345
http://www.materialsscience.pwr.wroc.pl/
DOI: 10.2478/msp-2021-0028

Stable aqueous dispersions of bare and double layer functionalized superparamagnetic iron oxide nanoparticles for biomedical applications

Jano Markhulia[1,*], Shalva Kekutia[1], Vladimer Mikelashvili[1], László Almásy[2], Liana Saneblidze[1], Tamar Tsertsvadze[3], Nino Maisuradze[3], Nino Leladze[3], Manfred Kriechbaum[4]

[1]Vladimer Chavchanidze Institute of Cybernetics of the Georgian Technical University, 0186 Tbilisi, Georgia
[2]Centre for Energy Research, Budapest, Hungary
[3]Ivane Javakhishvili Tbilisi State University, 0179 Tbilisi, Georgia
[4]Institute of Inorganic Chemistry, Graz University of Technology, Graz, Austria

Superparamagnetic iron oxide nanoparticles (SPIONs) have attracted the particular interest of scientists from various disciplines since their obtaining to the present day. The physicochemical and pharmacokinetic properties of SPIONs-containing magnetic nanofluids, and their applicability in biomedicine, largely depend on the stability of the colloidal system, particle size, size distribution, net magnetic moment, phase composition, and type and properties of stabilizers. Also, in some cases, when using magnetic nanoparticles for biomedical purposes, it is necessary that the stabilizing ligands of nanoparticles should not significantly change the magnetic properties. From this point of view, the preparation of stable colloidal systems containing bare iron oxide nanoparticles (BIONs) in water at physiological pH attracts particular attention and becomes increasingly popular in scientific circles. This study is focused on the development of the synthesis of aqueous suspensions of SPIONs stabilized with various organic molecules (oleic acid [OA] and poly(ethylene glycol) monooleate - with molecular weights 460 and 860) using a modified controlled chemical coprecipitation reaction, as well as stable nanofluids containing BIONs in an aqueous medium at neutral pH (near-physiological). The obtained samples were characterized using X-ray diffraction (XRD), Fourier Transform Infrared Spectroscopy, small-angle x-ray scattering (SAXS), dynamic light scattering (DLS), electrophoretic light scattering (ELS), and Vibrating Sample Magnetometry.

Keywords: *SPIONs, bare iron oxide nanoparticles, Poly (ethylene glycol) monooleate, oleic acid, ferrofluids*

1. Introduction

Nanocomposite materials based on superparamagnetic iron oxide nanoparticles (SPIONs), in particular the magnetic nanofluids, represent a special category of smart nanomaterials that open up promising prospects both for the scientific-technical applications, as described in the review paper by Vekas [1], as well as biomedical fields, especially in the area of diagnostic and therapeutic applications, as reported in the review by Genchi et al. [2]. The specific research interest in suspensions of magnetic nanoparticles in appropriate carrier liquids is due to the variety of properties of these nanocomposites – such as structural and orientational phase transitions, complex hydrodynamics, and thermal characteristics, as investigated by numerical calculations by Abdi et al. [3], as well as strong changes in their physical properties in moderate magnetic fields, demonstrated by Szalai and Dietrich, who calculated in mean field approximation the phase transitions and phase behavior of confined dipolar fluids [4].

The physicochemical and pharmacokinetic properties of ferromagnetic nanofluids, as well as their application for biomedical purposes, largely depend on the stability of the colloidal system, particle size, size distributions, net magnetic moment, crystal structure, phase composition, and type and properties of stabilizers (surfactants); these aspects are discussed thoroughly in the review paper by

* E-mail: j.markhulia@gtu.ge

Liang and co-workers [5]. Magnetic nanoparticles should have specific complex properties when used in biomedical applications. Thus, they should possess biocompatibility, and the ability to not aggregate and sediment in aqueous media [5].

The nature of ligands covering the surface of nanoparticles is an important factor determining their colloidal stability or toxic effect in biosystems. The selection of suitable surface ligands for specific nanoparticles, taking into account the properties of the dispersion medium, not only ensures sedimentation and aggregative stability of the colloid but also can impart lyophilic or lyophobic characteristics and chemical functionality to nanoparticles. To achieve this, the ligand molecules must be bonded to the surface of the nanoparticles through some kind of attractive interaction, for example, chemisorption, electrostatic attraction, or hydrophobic interaction. In a recent review, Walter et al. summarized the various methods of iron oxide nanoparticle functionalization that can make them suitable for *in-vivo* biomedical applications [6].

Therefore, for the efficient use of nanoparticles, strategies for attaching various types of ligands to the surface of nanoparticles are developed. The choice of the suitable ligands is crucial to satisfactorily address conditions such as the dispersion medium, the ion concentration, and the nature of the interaction, which can cause the dissociation of nanoparticles. Das et al. studied nanoparticles capped with single layers and bilayers formed by oleate, polyethylene glycol ligands, and their combinations, and revealed good stability and non-toxicity of the bilayer capped particles. However, the dissociation of the bilayer may have left open the hydrophobic oleate layer, causing increased toxicity to the cells [7].

Among the pathways for obtaining water-soluble functionalized iron oxide nanoparticles (IONPs) is their modification with biocompatible organic molecules. This approach is advantageous since both electrostatic and steric stabilization are jointly involved in sedimentation and aggregate stability of the colloidal system, while providing biocompatible coating functions for subsequent conjugation with various biomolecules. The advantage of electrostatic stabilization over polymeric (steric) stabilization is reversibility from the aggregated state by dilution. Such an approach has been used by De Sousa et al., using citrate-coated magnetite for magnetic hyperthermia [8]. However, the coating of the iron oxide surface with large organic molecules affects their hydrodynamic behavior. Therefore, it is important to note the effects arising from synthesizing IONPs by chemical coprecipitation and modifying their surface with small organic molecules with a high ability to deprotonate, which leads to electrosteric stabilization [8].

To obtain a stable colloid of IONPs, long-chain hydrocarbons containing coordination groups such as $C_{18}H_{34}O_2$ – oleic acid (OA) are often used [8]. When the surface of IONPs is modified with OA molecules, they form hydrophobic monolayers [1, 8]. Such single surfactant layer-covered IONPs can be easily dispersed in a non-polar dispersion medium, as done for example in the study by Vekas [1]. However, for biological use, complete dispersion of IONPs in an aqueous medium is required. Subject to the appropriate conditions in the synthesis/modification of magnetic IONPs, it is possible to obtain a bilayer oleic coating around nanoparticles that are well dispersed in water, and the coating conditions can be optimized for achieving an optimum colloidal stability, as shown by Lai et al. [9], who modified the amount of loaded OA in the double-shell coated nanoparticles in basic aqueous medium.

Depending on the requirements for individual parameters (toxicity, stability, etc.) it is sometimes necessary to completely or partially replace these secondary layers [7, 10]. For this, it is convenient to additionally modify IONPs with amphiphilic molecules, such as polyethylene glycol derivatives (PEG-derivatives) – in particular, with poly(ethylene) glycol monooleate (PEGMO) [11, 12]. This approach is justified, especially for targeted drug delivery, since drug-carrier nanoparticles modified with PEG-derivatives and having functional groups exhibit the best desirable properties [13]. In addition, the hydrophobic PEGMO chain can hydrophobically interact with OA molecules, thus forming a secondary layer on the surface of magnetic nanoparticles modified

with OA, and the hydrophilic head of the molecule enters the dispersed medium, making the particle dispersible in water [11].

As mentioned above, surface modification is a necessity due to the propensity of IONPs to agglomerate in an aqueous dispersion medium. It serves to achieve colloidal stability over the long term. However, coating the surface of magnetic nanoparticles with different materials has both positive and negative sides. In particular, modification of the surface of IONPs with organic and inorganic molecules often leads to physicochemical lability and changes in magnetic properties (a decrease in the average magnetic moment due to the presence of a diamagnetic membrane), and sometimes even to a decrease in the stability of the colloid. In addition, the modification of magnetic nanoparticles using various types of molecules is a complex and laborious process associated with additional costs, while the hydrodynamic sizes of nanoparticles in the dispersion medium increase. Many issues concerning the surface functionalization for applications in biomedicine and environment remediation have been discussed in a recent review by Magro and Vianello [14]. In some cases, when using magnetic nanoparticles for biomedical purposes (magnetic hyperthermia, bioseparation, MRI diagnostics, etc.), it is necessary that the stabilizing ligands of nanoparticles should not significantly change the magnetic properties. From this point of view, the preparation of stable colloidal systems containing bare iron oxide nanoparticles (BIONs) in water at physiological pH attracts particular attention and becomes increasingly popular in scientific circles with the prospect of their application in bionanotechnology. This direction has been less studied due to the novelty of the issue; Therefore, the discovery of new properties of pristine iron oxide surfaces and the production of colloidal liquids based on them, stable in physiological pH, is of particular importance [14, 15].

The present study aims to obtain water-based nanofluids containing double-layer functionalized (OA and PEGMO) SPIONs using a modified controlled chemical coprecipitation reaction (with a selection of optimal synthesis conditions), as well as stable nanofluids containing BIONs in an aqueous medium at near-physiological pH. Comprehensive experimental studies of the physical characteristics (magnetization, size, size distribution, crystal structure, phase composition) of the obtained materials were carried out.

2. Materials and methods

2.1. Materials and reagents

All analytical reagents required for the synthesis were used without further purification. For the synthesis of magnetic nanofluids containing BIONs, as well as nanoparticles coated with organic molecules (OA, poly(ethylene glycol) monooleate average Mn ~ 460 – $PEGMO_{460}$, poly(ethylene glycol) monooleate average Mn ~ 860 – $PEGMO_{860}$) we used: iron (III) chloride hexahydrate ($FeCl_3 \cdot 6H_2O$) ($\geq$ 98% – Sigma-Aldrich, Germany), iron (II) sulfate heptahydrate ($FeSO_4 \cdot 7H_2O$) ($\geq$ 99% – Carl Roth Gmbh + Co. KG, Germany), solution of ammonium hydroxide (NH_4OH) ($\geq$ 25% – Carl Roth Gmbh + Co. KG – Germany), OA (technical grade, 90% Sigma-Aldrich – Germany), $PEGMO_{460}$ (Sigma-Aldrich, Germany), $PEGMO_{860}$ (Sigma-Aldrich – Germany). The distilled water was used during the whole process of synthesis.

2.2. Preparation of magnetic nanofluids containing SPIONs

Water-based magnetic nanofluids containing bare IONPs as well as OA-coated IONPs, and subsequently modified by PEGMO (OA-SPIONs, OA-PEGMO-SPION), were obtained by modifying a standard chemical coprecipitation procedure, and by performing the controlled coprecipitation in a reactor under a low-vacuum environment (1 kPa). The vacuum environment was used to prevent the undesired oxidation of divalent iron ions (Fe^{2+}).

Two independent syntheses were performed in the present study: magnetic nanofluids containing bare IONPs at close to physiological pH were obtained in Synthesis 1, while in Synthesis 2, IONPs were coated with OA and modified by OA–$PEGMO_{460}$ and OA–$PEGMO_{860}$. Both syntheses are described in detail below.

2.2.1. Synthesis 1 (Synthesis of magnetic nanofluids containing BIONs)

The whole synthesis process can be divided into the following stages:

Stage I – Synthesis of a ferromagnetic fluid containing BIONs:

In the chemical reactor 0.044 mol of $FeCl_3 \cdot 6H_2O$ was dissolved in distilled water at 45°C, in a vacuum environment and stirred by a magnetic stirrer for 30 min. At the same time, 0.024 mol $FeSO_4 \cdot 7H_2O$ was dissolved in distilled water at 45°C, in a vacuum environment with mechanical stirring for 30 min. Also, separately 26 mL of 25% ammonium hydroxide (NH_4OH) was dissolved in 66 mL distilled water with magnetic stirring at 40°C for 30 min. After complete dissolution, 0.2 molar aqueous solution of iron (III) chloride was added to 0.2 molar aqueous solution of iron (II) sulfide in the chemical reactor by peristaltic pump. The mixture of iron salts was stirred with a mechanical stirrer (750 rpm) for 10 min at 45°C, in a vacuum environment, followed by the addition of 0.2 molar ammonium hydroxide through a peristaltic pump resulting in a black colloidal solution that was further stirred for an additional 40 min (750 rpm, 45°C).

Stage II – washing, ultrasonic processing of the synthesized magnetic fluid:

The resulting black precipitate was washed with distilled water by decantation on a permanent magnet to remove residuals after reaction (ammonium chloride and sulfate) until the pH reached ~7. After washing, the black precipitate was filled with distilled water up to 450 mL and ultrasonicated for 5 min.

After that, the entire fluid was divided into two parts: one part was dried in a vacuum evaporator to obtain powder samples (for X-ray diffraction (XRD) and Fourier-transform infrared spectroscopy (FTIR) measurements), and another part was stored in a liquid form (for vibrating-sample magnetometer (VSM), Dynamic Light Scattering (DLS)/Electrophoretic Light Scattering (ELS), and Small-angle X-ray scattering (SAXS)). These samples were labeled as BIONs.

2.2.2. Synthesis 2 (Synthesis of magnetic nanofluids modified with $PEGMO_{460}$ and $PEGMO_{860}$)

In synthesis 2, BIONs was stabilized by OA during the synthesis in the same chemical reactor (like Synthesis 1) after precipitation and then additionally modified immediately (without washing) with $PEGMO_{460}$ and $PEGMO_{860}$ by ultrasonication. Synthesis was performed as follows:

First, 0.0218 moles of $FeCl_3 \cdot 6H_2O$ and 0.0114 moles of $FeSO_4 \cdot 7H_2O$ (Fe^{3+}/Fe^{2+} = 1.9) were separately dissolved in distilled water (218.28 mL and 114.8 mL, respectively) at 45°C, in a vacuum environment, with constant mechanical stirring at 450 rpm for 10 min. Then these liquids were mixed for 15 min in a chemical reactor at 750 rpm. 13 mL of 25% ammonium hydroxide NH_4OH was added dropwise using a peristaltic pump (rate: ≈ 1.05 mL/min). After ammonium hydroxide addition, stirring was continued at the same temperature and speed for 30 min in the vacuum.

After this, the stirring speed was reduced, and 0.41 mL (365 mg) of OA was added dropwise through a peristaltic pump. At the same time, the temperature was gradually increased to 60°C while the stirring was continued for 30 min; after that, the temperature control was turned off and the stirring went on for 90 min until the fluid cooled down to room temperature.

After the sonication of obtained nanofluid (processing time 30 min, power 100 W), a small part of the OA-stabilized magnetic colloid was removed for FTIR and XRD measurements and the rest was divided into two parts: one part for the stabilization by $PEGMO_{460}$ and the second part for $PEGMO_{860}$ using sonication. In both cases, 243 mg of the corresponding PEG-monooleate was dissolved into 5 mL of distilled water and added dropwise to the OA-stabilized colloid by the peristaltic pump during 10 min.

These obtained samples were washed by decantation on a permanent magnet until pH 7.8 was reached. The samples were named as: $PEGMO_{460}$-OA-SPIONs, $PEGMO_{860}$-OA-SPION, and OA-SPIONs.

2.3. Characterization techniques

2.3.1. DLS and ELS

The hydrodynamic measurements, including the ζ potential, were carried out using a Litesizer 500 particle analyzer (Anton Paar, Austria). The instrument had the following specifications: measuring range of nanoparticle sizes: from 0.3 nm to 10 μm; Zeta potential measurement range: $\pm$600 mV; angle of measurement 15°; and pH range from 2 to 12. A semiconductor laser (40 mW, 658 nm) was used as the light source.

2.3.2. XRD

The dry powders of the Bare-Fe_3O_4 (BIONs), OA-SPIONs, $PEGMO_{460}$-OA-SPIONs, $PEGMO_{860}$-OA-SPIONs were measured using a DRON 3M X-ray diffractometer, operating with Fe Kα radiation (λ = 1.937283 Å) filtered by a manganese foil, at the voltage of 35 kV and current of 15 mA. The scanning speed was 2 degree/min.

2.3.3. VSM

Magnetization curves of magnetic fluids of the samples BIONs, OA-SPIONs, $PEGMO_{460}$-OA-SPIONs, and $PEGMO_{860}$-OA-SPIONs were measured on a Vibrating Sample Magnetometer (Cryogenic Limited, UK) at room temperature under an applied field up to 3 Tesla. Vibrator ran at 21 Hz and 2 mm peak to peak amplitude. 0.15 mL of nanofluids with magnetic nanoparticles (with a solid phase concentration of 0.66 g/100 mL) were placed in special containers.

2.3.4. FTIR

The FTIR spectroscopy studies were done using an Agilent Cary 670 instrument on powder samples BIONs, OA-SPIONs, $PEGMO_{460}$-OA-SPIONs, and $PEGMO_{860}$-OA-SPIONs. The samples were mixed with KBr to form pellets, and the measurements were carried out in the air. FTIR spectra of a liquid form of pure OA, $PEGMO_{460}$, and $PEGMO_{860}$ were measured on a Thermo Scientific™ Nicolet™ iS™ 5 FT-IR spectrometer (Thermo Fisher Scientific, USA).

2.3.5. SAXS

SAXS measurements were carried out using the instrument SAXSpoint 2.0 (Anton Paar, Austria). Using Cu Kα radiation and a hybrid photon-counting 2D EIGER R series detector, it became possible to cover a q-range of 0.05–5.7 nm^{-1} with q-resolution $\delta q < 0.003$ nm^{-1}. The measurements were carried out on samples in solution at room temperature using quartz capillaries of 1 mm in diameter.

3. Results and discussion

3.1. ELS and DLS measurement

An effective indicator of the stability of a colloidal dispersion is Zeta-potential, the parameter associated with the surface charge of particles suspended in a dispersion medium [6, 16]. The experimental data for ELS and DLS study are collected in Table 1, while Figure 1 shows the distribution of the size and Zeta-potential of the synthesized samples.

As can be seen from Figure 1, the ζ potential of the magnetic nanofluid containing BIONs at pH = 7.0 is positive and its average value is 21 mV, although most scientific literature indicates that the zero-point charge (ZPC) for magnetite (Fe_3O_4) in the water dispersion medium is in the region of 6.5, and the isoelectric point (IEP) is observed at pH $\approx$ 6–6.8. Therefore, magnetite particles in an aqueous dispersion medium are losing stability and flocculated near this point due to the low density of the surface charge [17–19].

Thus, with an increase in pH above the IEP, the potential of bare magnetite in an aqueous dispersed medium turns negative due to deprotonation, and vice versa, at a low pH, the total charge is positive [6, 19].

However, in our case, bare magnetite-containing magnetic fluid near pH 7.0 does not have a low zeta potential and, accordingly, does not aggregate even for several months, which indicates its electrostatic stabilization. We believe that this is due to the following reason: as is known, magnetite nanoparticles exhibit amphoteric surface activity and are capable of forming charges on their

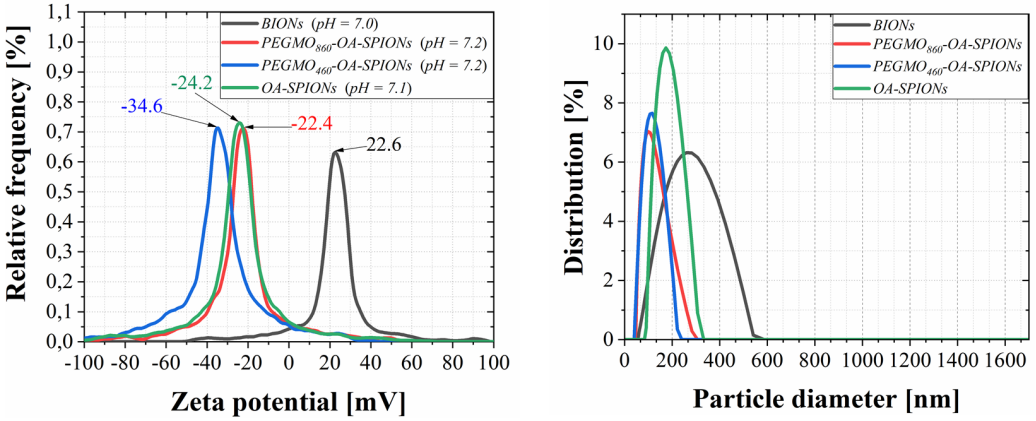

Fig. 1. The Zeta-potential and size distribution of particle agglomerates in the synthesized samples. BIONs, bare iron oxide nanoparticles; OA, oleic acid; PEGMO, poly(ethylene) glycol monooleate; SPIONs, superparamagnetic iron oxide nanoparticles.

Table 1. ELS and DLS Experimental results of samples.

Samples	Measurement temperature °C	Mean value of potential (mV)	Hydrodynamic diameter (nm)	Polydispersity index (%)
BIONs	20	21.7	225	20.6
OA-SPIONs	20	−24.2	182	22.0
$PEGMO_{860}$-OA-SPIONs	20	−23.3	101	19.5
$PEGMO_{460}$-OA-SPIONs	20	−34.5	110	23.2

BIONs, bare iron oxide nanoparticles; DLS, dynamic light scattering; ELS, electrophoretic light scattering; OA, oleic acid; PEGMO, poly(ethylene) glycol monooleate; SPIONs, superparamagnetic iron oxide nanoparticles.

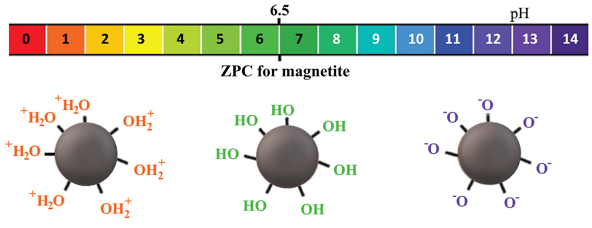

Fig. 2. Schematic representation of charges on the surface of magnetite nanoparticles as a function of pH. ZPC, zero-point charge.

surface by protonation of Fe – OH reaction centers (Fe – OH + H^+ Fe $–OH_2^+$) and deprotonation (Fe – OH Fe – O^- + H^+). These reactions on the surface can be interpreted as the specific adsorption of H^+ and OH^- ions on the interface of water – solid IONP (see Figure 2) [20].

Accordingly, depending on the pH of aqueous solution, magnetite has a positive or negative charged surface. In addition to pH value, the ionic strength of the dispersion medium (the presence of multivalent cations in the dispersion medium) also affects the ζ potential [17].

In our opinion, such a high value of the zeta potential (22 mV) in the pH $\approx$ 7 region is associated with the adsorption of divalent/trivalent iron ions (possibly divalent ions are turned to trivalent ions) remaining in the aqueous solution after the synthesis of nanoparticles. This results from the stoichiometry of the reaction mixture, since the ratio Fe^{+3}/Fe^{+2} = 1.84. The surface-bonded ions increase the ionic strength and the magnitude of the zeta potential.

A similar mechanism was suggested by Sun et al. [21]. They studied natural and synthetic magnetite of different compositions in aque-

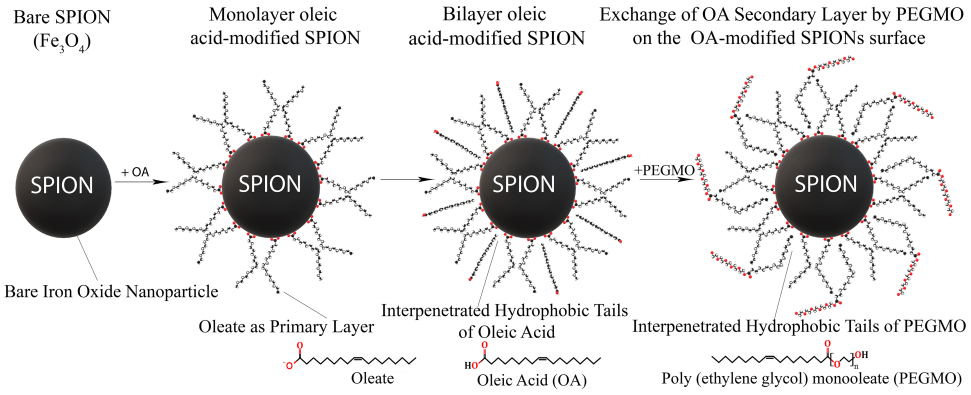

Fig. 3. Schematic depiction of the stabilization of Fe_3O_4 nanoparticles in water. OA, oleic acid; PEGMO, poly(ethylene) glycol monooleate; SPION, superparamagnetic iron oxide nanoparticles.

ous suspension, and found that in the presence of Fe^{+2} or Fe^{+3} cations, specific adsorption on the surface of magnetite nanoparticles, even in very small quantities, strongly affects the magnitude of the zeta potential.

Thus, a positive zeta potential with a magnitude of 22 mV in the region of pH = (6.5–7.0) leads to the sedimentation stability of nanofluid containing bare magnetite nanoparticles and indicates effective electrostatic stabilization, which also affected the hydrodynamic size of magnetite nanoparticles in a dispersion medium.

As for the samples OA-SPIONs, $PEGMO_{460}$-OA-SPIONs, and $PEGMO_{860}$-OA-SPIONs, their ζ-potential is −24.2, −23.3, and −34.5 mV, respectively (Figure 1). As described above in Synthesis 2, a magnetic nanofluid containing IONPs stabilized with OA was first prepared and then modified with PEG monooleate ($PEGMO_{460}$and $PEGMO_{860}$, respectively). Indeed, it is known that OA has a polar head of the carboxyl group and a non-polar hydrocarbon tail (Figure 3). It is also known that carboxylate anions coordinate on the surface of magnetite, preferably around iron atoms, with both carboxylate oxygen atoms (COO). Thus, the polar head is attached to the magnetite surface, and the nonpolar tail extends into dispersion medium; therefore, such single-layer coated magnetite nanoparticles are hydrophobic and well dispersible in organic solvents [22, 23]. In order for the OA coated magnetite nanoparticles to become hydrophilic, they must form a second shell. Such a shell is formed from free OA molecules (present in a disperse medium) by van der Waals forces. They coordinate with the hydrophobic tails around the first oleate layer so that the carboxyl head remains in the water phase, forming a hydrophilic bilayer around the nanoparticles (Figure 3). Thus, the coating of nanoparticles with OA molecules should lead to negative zeta potentials [24].

Apparently, in our case, the samples were completely coated with OA double shells. Thus, during the process of modifying magnetic nanofluid with PEGMO molecules, oleic molecules were replaced by PEG monooleate molecules in the outer layer, thereby completely encapsulating the nuclei of the magnetite NP with the formation of a two-layer hydrophilic shell, which leads to an electrostatic and steric stabilization (see Figure 3). This mechanism has also been confirmed by IR spectroscopy, as further explained below. The high zeta potential of these samples provides high colloidal stability of the colloidal system. The hydrodynamic dimensions of the samples are 101.5 nm and 108.9 nm, respectively.

3.2. XRD results

XRD patterns of the samples are shown in Figure 4. All diffraction patterns show the same characteristic reflections of the cubic crystal structure of the spinel: (220), (311), (400), (422), (511), (440), (533), (642), (731) (JCPDS No. 019-0629), at near to the following angles 2Θ (Cu Kα): 30, 35, 43, 53, 57, 63, 74, 87, 90, respectively.

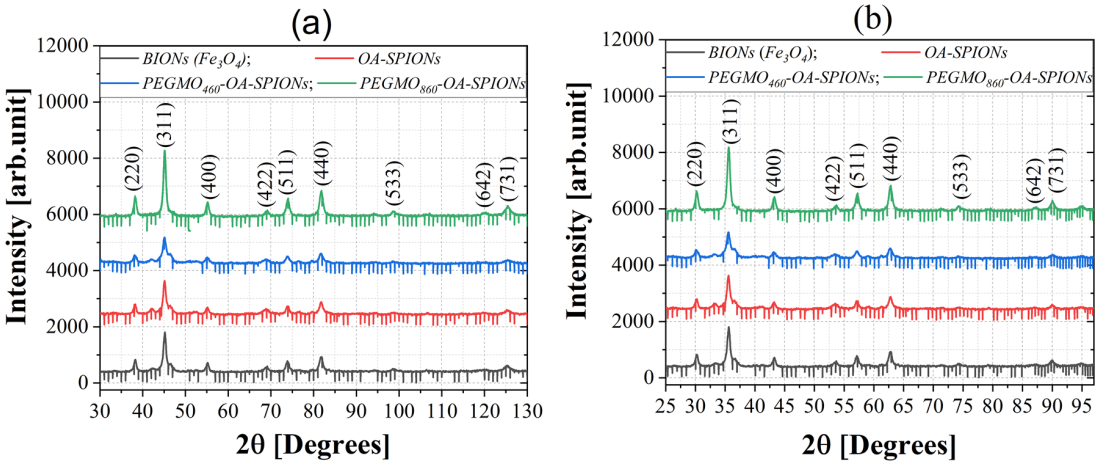

Fig. 4. Diffractograms of synthesized specimens taken with Fe Kα anode (λ = 1.937283 Å) (a), the same diffractograms converted to Cu Kα radiation (λ = 1.54178 Å) (b). BIONs, bare iron oxide nanoparticles; OA, oleic acid; PEGMO, poly(ethylene) glycol monooleate; SPIONs, superparamagnetic iron oxide nanoparticles.

Table 2. Average crystallite size of the samples calculated by Scherrer formula.

Sample	**Average size of crystallite estimated by XRD (Fe Kα; λ = 1.937Å) (nm)**	**Crystalline lattice parameter (Å)**
BIONs	20.0	8.3755
OA–SPIONs	21.8	8.3755
$PEGMO_{460}$–OA–SPIONs	21.0	8.3725
$PEGMO_{860}$–OA–SPIONs	23.1	8.3725

BIONs, bare iron oxide nanoparticles; OA, oleic acid; PEGMO, poly(ethylene) glycol monooleate; SPIONs, superparamagnetic iron oxide nanoparticles; XRD, X-ray diffraction.

It is known that magnetite and maghemite have the inverse spinel structure, and the difference between their permanent lattices is small. The lattice constant of magnetite, depending on the stoichiometry during the synthesis, as well as on the temperature treatment, varies between 8.348 and 8.396, while for maghemite it is 8.33–8.336 Å [21]. The lattice parameters of the synthesized samples correspond to the magnetite parameters (Fe_3O_4) (Table 2). The absence of other interference maxima indicates that the sample does not contain crystalline impurities. In addition, the dark black color and strong magnetic properties of dried powders of magnetic fluids are a hallmark of magnetite, in comparison with other iron oxides.

When the crystallite size of the sample does not exceed 150 nm, the width of the peak of XRD of the powders is inversely proportional to the size of the crystals. In this case, it is possible to calculate the effective crystallite sizes, which are close to the size of the nanoparticles. We calculated the effective dimensions of the crystalline grains using the Scherrer equation:

$$D = \frac{K\lambda}{\beta \cos\theta}$$

where D – average crystallite size; K – a dimensionless shape factor (Scherrer's constant), taken as 0.95 for spherical shape; λ – the X-ray wavelength (λ (Fe Kα) = 1.937283 Å; θ – diffraction angle (Bragg angle); and β – the line broadening at half the maximum intensity (FWHM) (in radians, and in 2θ units – Δ (2θ)). The calculated crystallite sizes are shown in Table 2.

3.3. SAXS measurement

The average size distribution of the particle agglomerates in the synthesized samples obtained by SAXS measurements is shown below. Data processing and modeling from the SAXS curve were performed as in our previous work, in which we prepared magnetite nanoparticles coated with folic acid using pulsed electrohydraulic discharges, in an automated chemical reactor [25].

It should be noted that the radiation scattering methods, in contrast to transmission electron microscopy, provide information on the size distribution of nanoparticles throughout the whole sample, and not for several hundred nanoparticles typically observed in TEM images. Thus, the results obtained by this method are integral characteristics and apply to the entire sample.

In order to get information about scattering of the particles only, extraction from scatter data was performed using the program Primus 3.3 [26]. Analysis of SAXS data such as radius of gyration (Rg) was carried out via Guinier fit; calculation of inverse Fourier transformations (IFTs) via GNOM was performed by a GUI based, open-source Python program BioXTAS RAW 2.0.3 [27]. Ab-initio shape determination by simulated annealing using a bead model was performed using DAMMIN [28]. These software packages have been developed by Svergun and co-workers at the European Molecular Biology Laboratory (EMBL) Group [26, 28].

The size distributions were calculated by the Monte Carlo regression package in McSAS software [29].

Figure 5 shows the scattering data in Guinier representation (ln I against q^2) for evaluating radius of gyration, Rg (Figure 6). Deviation from the linear behavior can indicate aggregation or a large polydispersity of the scattering particles.

Model parameter distributions in absolute volume fraction from the scattering data with reasonable uncertainty estimates were performed with software McSAS (Figure 7). The following parameter values were used: lower and upper q cut-off: 0.05–3.9 nm^{-1}, respectively; the number of repetitions: 10; model: sphere; and distribution of sphere

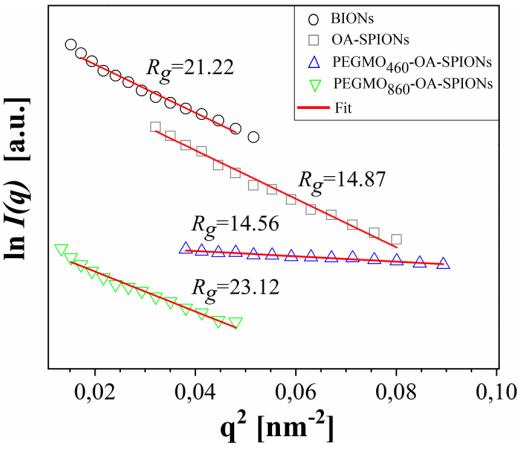

Fig. 5. Guinier plots for evaluating radius of gyration Rg for the colloid dispersions (the fitting of the reference model (red line) to experimental SAXS data (grey, blue, green). BIONs, bare iron oxide nanoparticles; OA, oleic acid; PEGMO, poly(ethylene) glycol monooleate; SPIONs, superparamagnetic iron oxide nanoparticles.

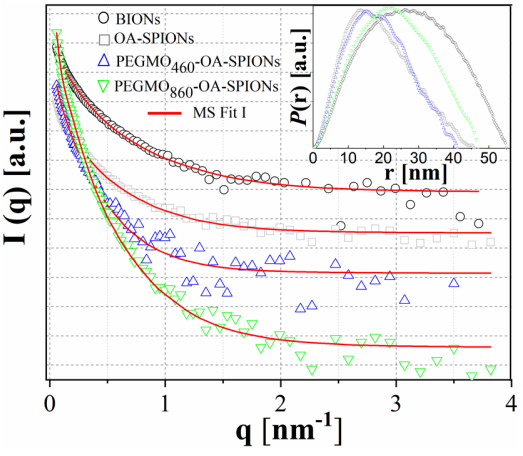

Fig. 6. McSAS fitting for evaluating size distribution and pair-distance distribution function p(r) obtained by GNOM. BIONs, bare iron oxide nanoparticles; OA, oleic acid; PEGMO, poly(ethylene) glycol monooleate; SPIONs, superparamagnetic iron oxide nanoparticles.

radii: between 1 nm and 60 nm. The red dashed line indicates the minimum level required for each bin to contribute in a measurable amount to the scattering pattern (i.e., the sensitivity limit).

The obtained distributions are nearly similar for all the samples, with some variations in the radius

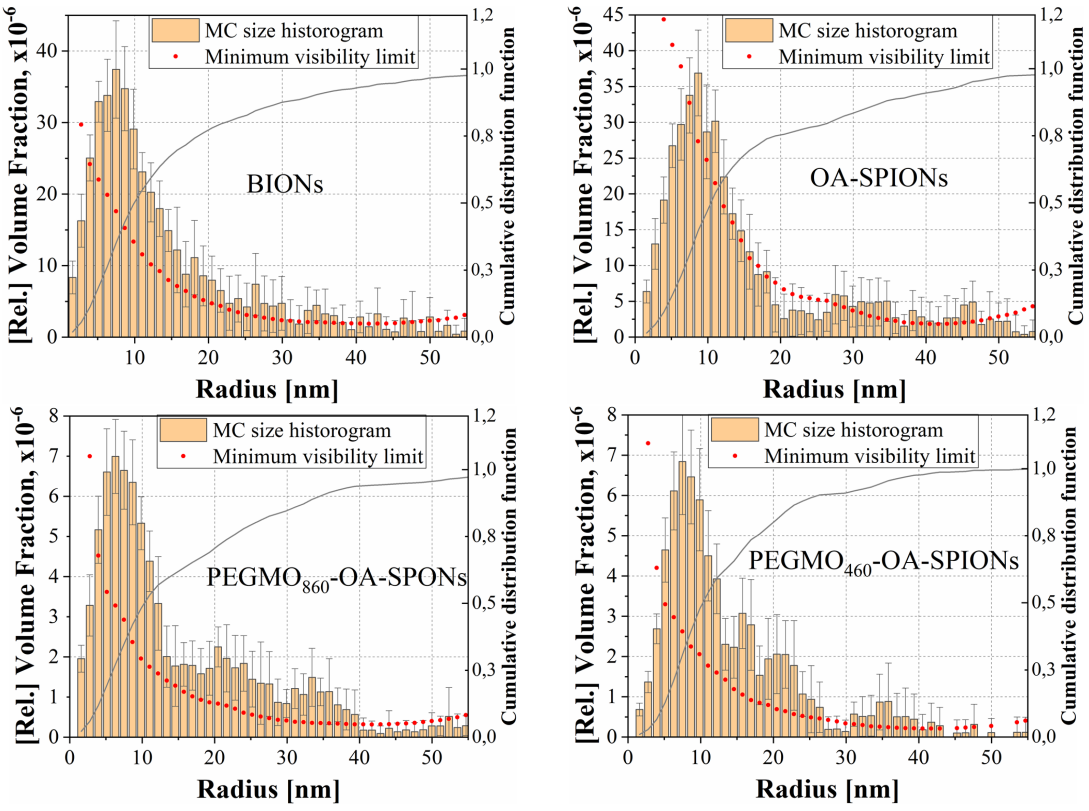

Fig. 7. Particle size distributions obtained using McSAS. BIONs, bare iron oxide nanoparticles; OA, oleic acid; PEGMO, poly(ethylene) glycol monooleate; SPIONs, superparamagnetic iron oxide nanoparticles.

Table 3. Nanoparticles average size obtained by SAXS measurement.

Sample	**Average radius of nanoparticles obtained by SAXS (nm)**
BIONs	14.6
OA–SPIONs	15.8
$PEGMO_{460}$–OA–SPIONs	14.0
$PEGMO_{860}$–OA–SPIONs	15.5

BIONs, bare iron oxide nanoparticles; OA, oleic acid; PEGMO, poly(ethylene) glycol monooleate; SAXS, small-angle X-ray scattering; SPIONs, superparamagnetic iron oxide nanoparticles.

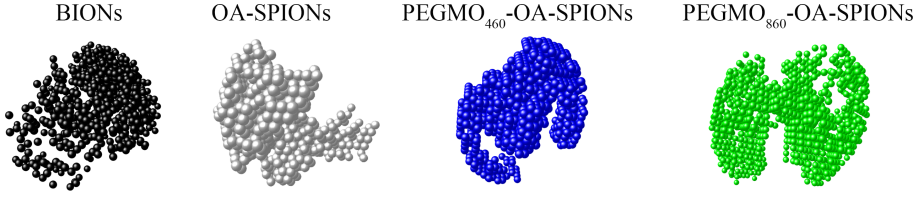

Fig. 8. Ab initio SAXS models of bare, OA-SPIONs, $PEGMO_{460}$-OA-SPIONs, and $PEGMO_{860}$-OA-SPIONs nanoparticles constructed using DAMMIN. OA, oleic acid; PEGMO, poly(ethylene) glycol monooleate; SAXS, small-angle X-ray scattering; SPIONs, superparamagnetic iron oxide nanoparticles.

range of 1–20 nm, and most of the particles have radii 6–10 nm, which is in good agreement with the single-particle or crystallite size obtained from the XRD data. The average size of particles and agglomerates, obtained by SAXS measurement, is shown in Table 3.

Using the output data of GNOM, we performed an ab-initio shape determination by simulated annealing using a single-phase dummy atom model (DAMMIN). The program restores ab-initio low-resolution shape of randomly oriented particles in solution (Figure 8). The reconstructed particle shapes resemble aggregates of nearly spherical particles.

3.4. Magnetometry measurements

Figure 9 shows the magnetization curves of the synthesized samples BIONs, OA-SPIONs, $PEGMO_{460}$-OA-SPIONs, and $PEGMO_{860}$-OA-SPIONs. As can be seen from the graph, no hysteresis loop was detected on the magnetization curves, which indicates that the ferromagnetic nanofluid contains single domain nanoparticles that exhibit superparamagnetism at room temperature.

In Figure 9, it is seen that for all samples at small values of the external magnetic field H_a, the magnetization increases rapidly with increasing magnetic field, reaching saturation at $H_a \approx 0.5$ T. The shape of the M(H) curves follow the Langevin magnetization behavior of superparamagnetic particles, as commonly observed for magnetite nanoparticles suspended in aqueous [30] and in oily [31] media.

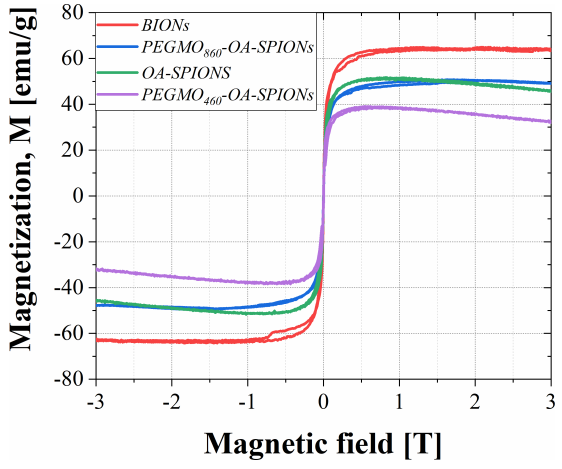

Fig. 9. Magnetization curves of synthesized samples at a temperature of 300 K. BIONs, bare iron oxide nanoparticles; OA, oleic acid; PEGMO, poly(ethylene) glycol monooleate; SPIONs, superparamagnetic iron oxide nanoparticles.

The saturation magnetization of the samples is given in Table 4. As expected, the BIONs sample has the highest value ($\approx$ 64 emu/g), while the samples modified with OA and PEG monooleate have lower saturation magnetization values.

It should be noted that the saturation magnetization value for the BIONs is less than the magnetization characteristic for bulk magnetite phase ($\mathbf{M}_s$ = 88 emu/g) [32]. The decrease in the saturation magnetization of the BIONs compared to the bulk phase can be explained by the surface effect, the so-called core-shell model of the magnetite nanoparticles. Indeed, a decrease in the size of nanoparticles sharply increases the number of atoms on the surface. The surface atoms have lower coordination numbers than intra-volume atoms, which leads to a violation of the lattice symmetry on the surface of nanoparticles, as well as to a violation of exchange bonds between surface spins, which in turn leads to spin disorder and, subsequently, to a general decrease in magnetism [33].

It is known that the effect of organic residues on the surface of nanoparticles contribute to the behavior of surface spins. This process can be interpreted as the effect of surface pinning. In fact, the

Table 4. Saturation magnetization of the samples.

Samples	**Saturation magnetization M_s (emu/g)**
BIONs (Fe_3O_4)	64.6 (H_a = 1.07 T)
OA-SPIONs	51.1 (H_a = 1.07 T)
$PEGMO_{460}$-OA-SPIONs	39.0 (H_a = 1.00 T)
$PEGMO_{860}$-OA-SPIONs	48.9 (H_a = 1.07 T)

BIONs, bare iron oxide nanoparticles; OA, oleic acid; PEGMO, poly(ethylene) glycol monooleate; SPIONs, superparamagnetic iron oxide nanoparticles.

field created by the ligand environment can cause the very strong pinning of magnetic moments on metallic ions in the surface layer, thereby affecting the magnetic properties [34].

Thus, compared to the BION sample, a decrease in the saturation magnetization of the samples modified with OA and PEG monooleate indicates that the magnetic nanoparticles are coated with organic molecules.

3.5. Analysis of FTIR spectra of the synthesized samples

In the FTIR spectrum of BIONs, a characteristic peak of magnetite is observed in the range 550–630 cm^{-1}; in our case, a peak at 580 cm^{-1} indicates the presence of magnetite with a face-centered, reverse spinel structure, which was also confirmed by X-ray analysis. In this range, the absorption band is due to vibrations of the Fe – O bonds in the tetrahedral and octahedral positions. The vibrational bands at 3,431 cm^{-1} and 1,630 cm^{-1}, corresponding to stretching (transverse) vibrations and O–H bending vibrations, are due to OH groups (coordinated on the surface of magnetite nanoparticles) and water molecules on unsaturated surface iron atoms [35].

The FTIR spectra of powder samples OA-SPIONs, $PEGMO_{460}$–OA–SPIONs, $PEGMO_{860}$–OA–SPIONs, and pure OA, $PEGMO_{460}$, $PEGMO_{860}$ in liquid form, are also presented in Figure 10.

In the FTIR spectrum in the range of 3,500–2,800 cm^{-1}, for all three powder samples, a wide absorption band was observed due to stretching vibrations of O–H bonds both in the carboxyl group (in the OA molecule) and in the hydroxyl group (coordinated around magnetite nanoparticles). In addition, the main peaks characteristic of pure OA was observed in the spectrum of the OA-SPIONs sample (Figure 10). In particular, the sharp peak (with low intensity) at 3,004 cm^{-1}, on which the band of stretching vibrations of O–H bonds is superimposed, is due to stretching vibrations of the C–H bond in the vinyl fragment [36], and peaks at 2,924 cm^{-1}, 2,855 cm^{-1}, and 1,459 cm^{-1} are caused by stretching (both symmetric and asymmetric) and deformation vibrations of (– CH_2–) bonds in the hydrophobic molecular chain of OA, respectively.

The average peak in intensity at 1,540 cm^{-1} is due to the symmetric stretching vibration of the carbon group [–COO–]. The sharp intense peak in the spectrum of pure OA at 1,707 cm^{-1} is associated with the C=O stretching vibration of the carbonyl group of OA molecules. This peak for the OA–SPIONs sample is shifted toward high wavenumbers (high energies) at 1,747 cm^{-1}, which clearly indicates that free OA molecules in the double layer around magnetite nanoparticles are connected by physical (hydrophobic) bonds with oleate molecules (primary layer) chemisorbed on the surface of IONPs (Figure 10).

This opinion is supported by the fact that, in contrast to the FTIR spectrum of pure OA, other peaks are also shifted in the spectrum of the OA-SPIONs sample; in particular, the absorption band at 1,289 cm^{-1}, which corresponds to stretching vibrations bond C–O, is shifted to the position of 1,240 cm^{-1}, and the peak at 935 cm^{-1} caused by the angular deformation of the bond (–CH_2–) is shifted by 894 cm^{-1}, respectively [37].

The above discussion of the existence of free OA molecules on a double layer around magnetite nanoparticles is confirmed by the fact that on the FTIR spectra of samples $PEGMO_{460}$–OA–SPIONs and $PEGMO_{860}$–OA–SPIONs, characteristic absorption bands of physically bounded OA molecules completely disappeared or significantly decreased.

In addition, there is a shift or the appearance of new bands. In particular, in the FTIR spectra of samples $PEGMO_{460}$–OA–SPIONs and $PEGMO_{860}$–OA–SPIONs, broad absorption bands appeared with an extremum at 3,140–3,141 cm^{-1}. This is most likely due to the superposition of the stretching vibrations of the OH group of pure magnetite and PEG monooleate molecules in this spectral band (characteristic bands of pure $PEGMO_{460/480}$ at 3,447/3,474 cm^{-1}, respectively). The absorption bands at 2,924 cm^{-1} and 2,855 cm^{-1} are shifted to 2,922 cm^{-1} and 2,852 cm^{-1}, respectively.

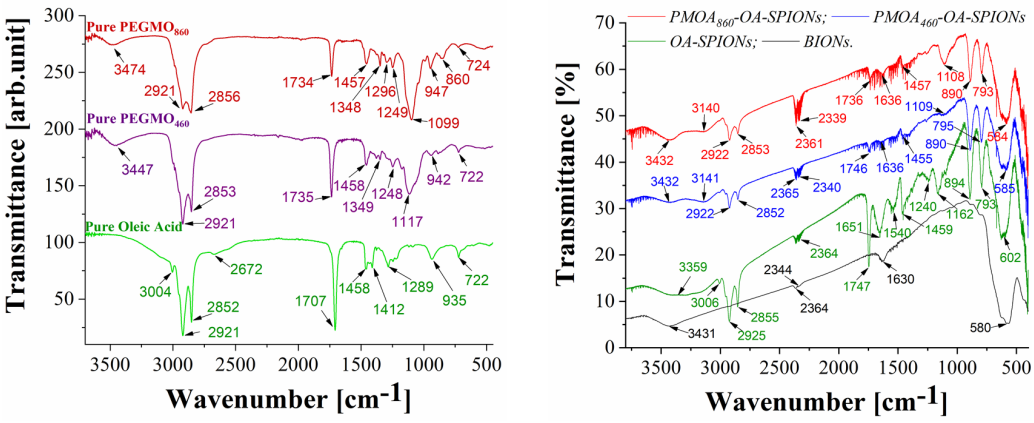

Fig. 10. FTIR spectra of pure OA, $PEGMO_{460}$, and $PEGMO_{860}$ in liquid form (left); FTIR spectra of BIONs, PEG_{460}-OA-SPIONs, and PEG_{860}-OA-SPIONs samples (right). BIONs, bare iron oxide nanoparticles; FTIR, fourier-transform infrared spectroscopy; OA, oleic acid; PEGMO, poly(ethylene) glycol monooleate; SPIONs, superparamagnetic iron oxide nanoparticles.

The displacement of the peaks is likely due to the physical interaction of PEG-monooleate with oleate molecules in the bilayer around magnetite nanoparticles.

In addition, a strong absorption band (at 1,117/1,099 cm^{-1}) and a characteristic absorption band at 1,735/1,734 cm^{-1} in the spectrum of pure $PEGMO_{460/860}$ (Figure 3), caused by the stretching vibration of the PEG ether group and by C = O stretching vibration [13], respectively, with small shifts at 1,109/1,108 cm^{-1} and 1,739/1,736 cm^{-1}, appear in both FTIR spectra of PEGMO-OA-SPION samples, respectively.

It should also be noted that when OA is chemisorbed on the surface of magnetite nanoparticles in the form of a carboxylate, COO- gives absorption band of C = O vibration at 1,635 cm^{-1} [38], which is observed for both samples. Thus, in the IR spectra of samples $PEGMO_{460}$ – OA-SPION and $PEGMO_{860}$ – OA-SPION, the slight shift of peaks of OA molecules and new peaks at 3,140/3,141, 1,636 cm^{-1} indicate chemisorbed oleate molecules on the surface of Fe_3O_4 nanoparticles.

4. Conclusions

In this study, we successfully synthesized magnetic nanofluids based on bare, OA, and PEG-monooleate modified magnetite nanoparticles by modification of the standard co-precipitation synthesis procedure in an automated chemical reactor.

The obtained water-based magnetic nanofluids (near physiological pH) containing bare magnetite nanoparticles retain sedimentation stability for months due to electrostatic stabilization. Such magnetic nanofluids can be used for biomedical purposes requiring high saturated magnetism and neutral aqueous pH.

Because of their good water solubility, biocompatibility, and the presence of functional groups, the obtained magnetic nanofluids modified with PEG derivatives (PEGMO) can be further functionalized with biomolecules or drugs and used in biomedicine.

Acknowledgements

This work was supported by Shota Rustaveli National Science Foundation of Georgia (SRNSFG) under GENIE project (Grant CARYS-19-976). The authors would like to acknowledge use of the Somapp Lab, a core facility supported by the Austrian Federal Ministry of Education, Science and Research, the Graz University of Technology, the University of Graz, and Anton Paar GmbH. The authors acknowledge the CERIC-ERIC Consortium for access to experimental facilities and financial support (Proposal no. 20177016).

References

[1] Vekas L. Magnetic nanofluids properties and some applications. Rom J Phys. 2004;49(9–10):707–21.

[2] Genchi GG, Marino A, Grillone A, Pezzini I, Ciofani G. Remote control of cellular functions: The role of smart nanomaterials in the medicine of the future. Adv Healthc Mater. 2017;6(9):1700002. https://doi.org/10.1002/adhm.201700002

[3] Abdi H, Motlagh SY, Soltanipour H. Study of magnetic nanofluid flow in a square cavity under the magnetic field of a wire carrying the electric current in turbulence regime. Results Phys. 2020;18:103224. https://doi.org/10.1016/j.rinp.2020.103224

[4] Szalai I, Dietrich S. Phase transitions and ordering of confined dipolar fluids. Eur Phys J E. 2009;28(3):347–59. https://doi.org/10.1140/epje/i2008-10424-2

[5] Liang YJ, Xie J, Yu J, Zheng Z, Liu F, Yang A. Recent advances of high performance magnetic iron oxide nanoparticles: Controlled synthesis, properties tuning and cancer theranostics. Nano Select. 2020;2(2):216–50. https://doi.org/10.1002/nano.202000169

[6] Walter A, Garofalo A, Parat A, Martinez H, Felder-Flesch D, Begin-Colin S. Functionalization strategies and dendronization of iron oxide nanoparticles. Nanotechnol Rev. 2015;4(6):581–93. https://doi.org/10.1515/ntrev-2015-0014

[7] Das GK, Stark DT, Kennedy IM. Potential toxicity of Up-converting nanoparticles encapsulated with a bilayer formed by ligand attraction. Langmuir. 2014;30(27):8167–76. https://doi.org/10.1021/la501595f

[8] De Sousa ME, Van Raap MBF, Rivas PC, Zélis PM, Girardin P, Pasquevich GA, et al. Stability and relaxation mechanisms of citric acid coated magnetite nanoparticles for magnetic hyperthermia. J Phys Chem C. 2013;117(10):5436–45. https://doi.org/10.1021/jp311556b

[9] Lai CW, Low FW, Tai MF, Hamid SBA. Iron oxide nanoparticles decorated oleic acid for high colloidal stability. Adv Polym Technol. 2018;37(6):1712–21. https://doi.org/10.1002/adv.21829

[10] Rahme K, Dagher N. Chemistry routes for copolymer synthesis containing peg for targeting, imaging, and drug delivery purposes. Pharmaceutics. 2019;11(7):327. https://doi.org/10.3390/pharmaceutics11070327

[11] Zhang X, Guo Z, Zhang X, Gong L, Dong X, Fu Y, et al. Mass production of poly(ethylene glycol) monooleate-modified core-shell structured upconversion nanoparticles for bio-imaging and photodynamic therapy. Sci Rep. 2019;9(1):5212. https://doi.org/10.1038/s41598-019-41482-w

[12] Zhang X, Tian G, Yin W, Wang L, Zheng X, Yan L, et al. Controllable generation of nitric oxide by near-infrared-sensitized upconversion nanoparticles for tumor therapy. Adv Funct Mater. 2015;25(20):3049–3056. https://doi.org/10.1002/adfm.201404402

[13] Xiong F, Li J, Wang H, Chen Y, Cheng J, Zhu J. Synthesis, properties and application of a novel series of one-ended monooleate-modified poly(ethylene glycol) with active carboxylic terminal. Polymer (Guildf). 2006;47(19):6636–41. https://doi.org/10.1016/j.polymer.2006.07.020

[14] Magro M, Vianello F. Bare iron oxide nanoparticles: Surface tunability for biomedical, sensing and environmental applications. Nanomaterials. 2019;9(11):1608. https://doi.org/10.3390/nano9111608

[15] Schwaminger SP, Fraga-García P, Blank-Shim SA, Straub T, Haslbeck M, Muraca F, et al. Magnetic one-step purification of his-tagged protein by bare iron oxide nanoparticles. ACS Omega. 2019;4(2):3790–9. https://doi.org/10.1021/acsomega.8b03348

[16] Oriekhova O, Stoll S. Investigation of FeCl3 induced coagulation processes using electrophoretic measurement, nanoparticle tracking analysis and dynamic light scattering: Importance of pH and colloid surface charge. Colloids Surfaces A. 2014;461:212–9. https://doi.org/10.1016/j.colsurfa.2014.07.049

[17] Laurent S, Forge D, Port M, Roch A, Robic C, Elst LV, et al. Magnetic iron oxide nanoparticles: Synthesis, stabilization, vectorization, physicochemical characterizations and biological applications. Chem Rev. 2008;108(6):2064–2110. https://doi.org/10.1021/cr068445e

[18] Yang XC, Shang YL, Li YH, Zhai J, Foster NR, Li YX, et al. Synthesis of monodisperse iron oxide nanoparticles without surfactants. J Nanomater. 2014;1–5. https://doi.org/10.1155/2014/740856

[19] Laurent S, Henoumont C, Stanicki D, Boutry S, Lipani E, Belaid S, et al. MRI contrast agents: From molecules to particles. Springer: Singapore; 2017.

[20] Tombácz E, Majzik A, Horvát ZS, Illés E. Magnetite in aqueous medium: Coating its surface and surface coated with it. Rom Rep Phys. 2006;58(3):281–6.

[21] Sun ZX, Su FW, Forsling W, Samskog PO. Surface characteristics of magnetite in aqueous suspension. J Colloid Interface Sci. 1998;197(1):151–9. https://doi.org/10.1006/jcis.1997.5239

[22] Shete PB, Patil RM, Tiwale BM, Pawar SH. Water dispersible oleic acid-coated Fe3O4 nanoparticles for biomedical applications. J Magn Magn Mater. 2015;377:406–10. https://doi.org/10.1016/j.jmmm.2014.10.137

[23] Jadhav NV., Prasad AI, Kumar A, Mishra R, Dhara S, Babu KR, et al. Synthesis of oleic acid functionalized Fe3O4 magnetic nanoparticles and studying their interaction with tumor cells for potential hyperthermia applications. Colloids Surfaces B. 2013;108:158–68. https://doi.org/10.1016/j.colsurfb.2013.02.035

[24] Liu X, Kaminski MD, Guan Y, Chen H, Liu H, Rosengart AJ. Preparation and characterization of hydrophobic superparamagnetic magnetite gel. J Magn Magn Mater. 2006;306(2):248–53. https://doi.org/10.1016/j.jmmm.2006.03.049

[25] Mikelashvili V, Kekutia S, Markhulia J, Saneblidze L, Jabua Z, Almásy L, et al. Folic acid conjugation of magnetite nanoparticles using pulsed electrohydraulic discharges. J Serbian Chem Soc. 2021;86(2):181–94.

https://doi.org/10.2298/JSC200414053M

[26] Konarev PV, Volkov VV, Sokolova AV, Koch MHJ, Svergun DI. PRIMUS: A Windows PC-based system for small-angle scattering data analysis. J Appl Crystallogr. 2003;36(5):1277–82. https://doi.org/10.1107/S0021889803012779

[27] Hopkins JB, Gillilan RE, Skou S. BioXTAS RAW: Improvements to a free open-source program for small-angle X-ray scattering data reduction and analysis. J Appl Crystallogr. 2017;50(5):1545–53. https://doi.org/10.1107/S1600576717011438

[28] Svergun DI. Restoring low resolution structure of biological macromolecules from solution scattering using simulated annealing. Biophys J. 1999;76(6):2879–86. https://doi.org/10.1016/S0006-3495(99)77443-6

[29] Bressler I, Pauw BR, Thünemann AF. McSAS: Software for the retrieval of model parameter distributions from scattering patterns. J Appl Crystallogr. 2015;48(3):962–9. https://doi.org/10.1107/S1600576715007347

[30] Maldonado-Camargo L, Unni M, Rinaldi C. Magnetic characterization of iron oxide nanoparticles for biomedical applications. Methods Mol Biol. 2017;1570:47–1. https://doi.org/10.1007/978-1-4939-6840-4_4

[31] Almásy L, Creanga D, Nadejde C, Rosta L, Pomjakushina E, Ursache-Oprisan M. Wet milling versus coprecipitation in magnetite ferrofluid preparation. J Serbian Chem Soc. 2015;80(3):367–76. https://doi.org/10.2298/JSC140313053A

[32] Huang Z, Tang F. Preparation, structure, and magnetic properties of mesoporous magnetite hollow spheres. J Colloid Interface Sci. 2005;281(2):432–6. https://doi.org/10.1016/J.JCIS.2004.08.121

[33] Pacakova B, Kubickova S, Reznickova A, Niznansky D, Vejpravova J. Spinel ferrite nanoparticles: Correlation of structure and magnetism. Magn Spinels - Synth Prop Appl. 2017:3–30. https://doi.org/10.5772/66074

[34] Sathish S, Balakumar S. Influence of physicochemical interactions of capping agent on magnetic properties of magnetite nanoparticles. Mater Chem Phys. 2016;173:364–71. https://doi.org/10.1016/j.matchemphys.2016.02.024

[35] Iyengar SJ, Joy M, Ghosh CK, Dey S, Kotnala RK, Ghosh S. Magnetic, X-ray and Mössbauer studies on magnetite/maghemite core-shell nanostructures fabricated through an aqueous route. RSC Adv. 2014;4(110):64919–29. https://doi.org/10.1039/c4ra11283k

[36] Premaratne WA, Priyadarshana WM, Gunawardena SH, De Alwis AA. Synthesis of nanosilica from paddy husk ash and their surface functionalization. J Sci Univ Kelaniya Sri Lanka. 2014;8:33–8. https://doi.org/10.4038/josuk.v8i0.7238

[37] Kumar TV, Prabhakar S, Raju GB. Adsorption of oleic acid at sillimanite/water interface. J Colloid Interface Sci. 2002;247(2):275–81. https://doi.org/10.1006/jcis.2001.8131

[38] Lu C, Bhatt LR, Jun HY, Park SH, Chai KY. Carboxylpolyethylene glycol-phosphoric acid: A ligand for highly stabilized iron oxide nanoparticles. J Mater Chem. 2012;22(37):19806–11. https://doi.org/10.1039/c2jm34327d

Received 2021-08-16
Accepted 2021-10-19